Materials Today Energy 30 (2022) 101186

Contents lists available at ScienceDirect

Materials Today Energy

journal homepage: www.journals.elsevier.com/materials-today-energy/

Accelerated radiation tolerance testing of Ti-based MAX phases

Matheus A. Tunes [a, *], Sean M. Drewry [b], Jose D. Arregui-Mena [c], Sezer Picak [a], Graeme Greaves [d], Luigi B. Cattini [e], Stefan Pogatscher [e], James A. Valdez [a], Saryu Fensin [a], Osman El-Atwani [a], Stephen E. Donnelly [d], Tarik A. Saleh [a], Philip D. Edmondson [f, g]

[a] Materials Science and Technology Division, Los Alamos National Laboratory, USA
[b] Department of Materials Science and Engineering, University of Tennessee, Knoxville, USA
[c] Materials Science and Technology Division, Oak Ridge National Laboratory, USA
[d] School of Computing and Engineering, University of Huddersfield, United Kingdom
[e] Chair of Non-Ferrous Metallurgy, Montanuniversitaet Leoben, Austria
[f] Department of Materials, The University of Manchester, United Kingdom
[g] Photon Science Institute, The University of Manchester, United Kindgom

ARTICLE INFO

Article history:
Received 31 August 2022
Received in revised form
17 October 2022
Accepted 18 October 2022
Available online 28 October 2022

Keywords:
MAX phases
Extreme environments
Neutron irradiation
Ion irradiation
In situ Transmission electron microscopy

ABSTRACT

MAX phases have recently attracted significant attention for potential nuclear applications due to their novel properties such as unique hexagonal-compact nanolayered crystal structure, high-machinability due to lower hardness levels than conventional ceramics, and high-chemical inertness. In order for MAX phases to be used in nuclear reactors, two aspects deserve detailed investigations: (i) their phase stability at high-temperatures and (ii) microstructural defect formation and recovery induced by energetic particle irradiation. To date, degradation mechanisms of MAX phases at high-temperatures and following irradiation are largely unexplored fields of research. This work focuses on the evaluation of two Ti-based MAX phases—Ti_2AlC and Ti_3SiC_2—within the context of extreme environments. To accomplish this, a one-of-a-kind comparison between neutron irradiations, performed over a decade of research at the high flux isotope reactor, and heavy-ion irradiations, carried out *in situ* in a transmission electron microscope, has been conducted. The results show Ti-based MAX phases are prone to accelerated decomposition under the conditions investigated. This questions the hypothesis that MAX phases exhibit high phase stability, especially when used in future nuclear energy systems where energetic particle irradiation is a dominating degradation mechanism.

1. Introduction

A new class of materials that are currently under investigation as potential structural materials for applications in extreme environments such as fission and fusion nuclear reactors are the $M_{n+1}AX_n$ phases (or simply MAX phases). Firstly synthesized by Jeitschko and Nowotny et al. circa 1960s in Austria [1–5] and revisited by Barsoum in the United States in the 1990s, who consolidated the literature in the field at the time [6,7], the MAX phases comprise a unique class of nanolayered carbide and nitride materials that can be formed via a specific stoichiometric rule—the $M_{n+1}AX_n$—where M is an early transition metal, A as an element from Group 13 or 14 of the periodic table, and X either C or N atoms [8]. The unique hexagonal-compact crystal structure of these compounds is derived by the intercalation between M_2X and A layers at the atomic scale, thus forming a nanostructured and nanolayered material with translational symmetry.

Scientists have resorted to the unique crystal structure and atomic arrangement of MAX phases to shed light on many of their reported extraordinary properties. On their mechanical behavior, it is often reported that MAX phases are softer than most conventional ceramics (*e.g.* MX ceramics such as TiN, ZrC) with hardness levels around 2–8 GPa making them less brittle and readily machinable [9–11]. Pseudo-ductility at high-temperatures has been reported due to the activation of basal slip systems, but in general, their characteristic brittle nature is restored at lower temperatures [10]. Regarding the physico-chemical aspect, MAX phases comprise a unique combination of metallic, covalent, and ionic bonding with the hybridization phenomena occurring between *p* and *d* quantum-mechanical orbitals of the constituent A

* Corresponding author.
E-mail address: tunes@lanl.gov (M.A. Tunes).

https://doi.org/10.1016/j.mtener.2022.101186

and M atoms, respectively [10]. High electrochemical resistance has also been attributed to different MAX phases, which can outperform existing materials in applications where corrosion resistance is a major concern [12,13].

This combination of unique elastic behavior, nanolayered crystal structure, high corrosion resistance, high-temperature properties, and presumably high thermodynamic stability [11] indicate that MAX phases could be potential candidates for future applications in nuclear technology, particularly for high-temperature reactor applications [14]. For their use in irradiation environments, MAX phases require further studies addressing how energetic particle irradiation modifies their crystal structure and how this damage forms, evolves and undergoes recovery within the microstructure of these materials. To date, two methodologies have been used to assess the irradiation response of MAX phases: neutron irradiation at materials test reactors and ion irradiation using particle accelerators [15–17].

The existing dataset on the irradiation response of MAX phases is still fairly scarce, with recent experiments performed at the MIT Nuclear Reactor Laboratory, Idaho National Laboratory's advanced test reactor and at Oak Ridge National Laboratory's (ORNL) high flux isotope reactor (HFIR) on bulk-synthesized MAX phases. Below is a brief summary of the neutron irradiation effects on MAX phases available in current literature:

- Ti_3SiC_2, Ti_3AlC_2, Ti_2AlC, and Ti_2AlN were irradiated up to 0.1 displacement-per-atom (dpa) at both 633 and 968 K. Phase decomposition due to neutron irradiation was reported to occur for all the MAX phases investigated: the MAX phases decomposed into binary transition carbides and nitrides, *i.e.* TiC (for the C-containing ones) and TiN (for the Ti_2AlN). No amorphization was observed within the dose and temperature range investigated. Evidence for the recovery of point defects was presented for the irradiations at 968 K assessed via electrical resistivity measurements [18].
- Ti_3SiC_2 and Ti_2AlC were further investigated up to 0.4 dpa at 633 K in the same study [18]. Displacement damage such as black-spots and small basal dislocation loops were detected within the microstructures. Micro-cracks were also present in the Ti_2AlC, but not in the Ti_3SiC_2. The presence of impurities as secondary phases—such as TiC and Al_3O_2—were observed to exhibit worse irradiation response than the MAX phase matrices. It was highlighted that Ti_3SiC_2 could be a potential candidate for nuclear applications due to the lower yield of defects observed in its damaged microstructure [19].
- Both Ti_3SiC_2 and Ti_3AlC_2 were subsequently investigated in the temperature ranging from 394 to 1321 K up to a maximum dose of 3.4 dpa. The detection of displacement damage in the form of black-spots and basal dislocation loops was confirmed in the irradiations at 1008 K, including the detection of stacking faults. Extensive void formation was reported in the materials irradiated at 1321 K, yet matrix grains less than 3–5 μm were observed to be free of damage. The active role of A-layers was proposed to be the origin for the suppression of irradiation damage formation in these materials. A general consensus was established toward the Ti_3SiC_2 as an appropriate MAX phase candidate material for nuclear applications up to 3.4 dpa and temperatures around 973 K [20].
- Ti_3SiC_2 and Ti_2AlC were irradiated with neutrons at 1273 K to two different neutron doses: 2 and 10 dpa, with the latter being the highest dose ever achieved with neutrons for MAX phases. A range of irradiation damage defects were reported, including black-spots accumulation observed to increase from 2 to 10 dpa, formation of extensive disordered dislocation networks, cavities, and <a> type dislocation loops. Both MAX phases experienced significant irradiation-induced phase decomposition and precipitation at 10 dpa, and although no evidence for amorphization was presented, the thermodynamic stability of these two Ti-based MAX phases in nuclear reactors was questioned [21].

Ion irradiation-based studies of defect formation and recovery in different MAX phases (beyond the Ti-based spectrum) were also investigated, including materials in bulk and thin solid film forms. These experiments were carried out with a broad variety of ion beam species and energy, dose, temperatures making comparison challenging, and as such a compilation represents a broad, non-exhaustive, overview of the ion irradiation effects in MAX phases [22–32]:

- Minor evidence for amorphization at doses around 25 dpa was noted for Ti-based MAX phases at 300 K [22]. Complete amorphization was observed for phase pure Cr_2AlC irradiated at 300 K up to 3.3 dpa [28]; conversely, a semi-crystalline (crystalline, but with amorphous nano-zones) Cr_2AlC irradiated at 623 K up to 40 dpa did not exhibit any amorphization [32]. At room temperature and around 3.5 dpa, partial amorphization of a Zr_2AlC MAX phase was discovered by Qarra et al. [29], but the Zr-based MAX phase remained fully crystalline under irradiation at higher temperatures (973 K) and same dose. The latter study also reported an increase in the density of dislocations and stacking faults constrained to the basal plane.
- Micro-cracks (similarly to those observed in neutron irradiations [19]) and phase decomposition were reported in Ti_3SiC_2 under heavy ion irradiation up to 10.3 dpa. Post-irradiation annealing of the irradiated specimens yielded evidence for recrystallization within the range of 773–1073 K [25]. Micro-cracks were also reported at around 3.5 dpa for the Zr_2AlC MAX phase [29].
- Anisotropic swelling (*i.e.* expansion of the c-axis and contraction of the a-axis) has been observed for the Ti_3SiC_2 under heavy irradiation with Kr and Xe [24,33] for doses lower than 30 dpa and at temperatures between 298 and 773 K. This swelling accompanied an increase of the MAX phase hardness and loss of the nanolamellar structure, with amorphization also observed under these irradiation conditions. Similar results for c-axis expansion were obtained by Liu et al. [23] in a 'quaternary' MAX phase, the $Ti_3(Si_{0.9}Al_{0.1})C_2$. Conversely, light-ion irradiations (He^+ ions) were used to assess the irradiation response of a double solid solution MAX phase, the $(Ti_{0.5},Zr_{0.5})(Al_{0.5},Sn_{0.5})C$. Although He platelets and extensive dislocation loop formation was reported, post-irradiation characterization using a high-resolution transmission electron microscope (TEM) revealed no disruption of the nanolamellar atomic structure characteristic of MAX phases [31], suggesting it to be an irradiation effect resulting from heavy-ions only.
- Self-healing of irradiation damage defects was suggested for some MAX phases under ion irradiation. This was proposed to be the result of an enhanced recombination of point defects due to lower energies for defect migration and Frenkel recombination [26,30–32].
- Following the results from neutron irradiation, an overall trend within the ion beam community also suggested Ti_3SiC_2 as the most prominent candidate material for nuclear applications.

In order to further evaluate the future applicability of Ti-based MAX phases in extreme radiation environments, an investigation consisting of both neutron and ion irradiation experiments has been conducted on two select Ti-based MAX phases: Ti_3SiC_2 and

Ti_2AlC. The main objective of this present study is to characterize and understand the resistance of Ti-based MAX phases when exposed to energetic particle irradiation, with particular interest on possible microstructural modifications, defect formation and recovery, and the bulk thermodynamic stability. Both candidate materials were irradiated with neutrons up to 2 and 10 dpa in the HFIR at a temperature of 1273 K and up to 5 dpa using a Kr ion beam *in situ* within a TEM in the microscope and ion accelerators for materials investigations (MIAMI-2) facility at a temperature of 1008 K. Prior to ion irradiation, an *in situ* TEM characterization study was also performed on the effects of thermal annealing in the microstructure of both materials when exposed to high-temperatures (1273 K). Additionally, the ion irradiation experiments on the Ti-based MAX phases were compared and contrasted with the pure metal constituents, α-Al and α-Ti, so that the underlying physical differences between the complex ceramics and their single element metal counterparts are presented and placed into context relating to the radiation response.

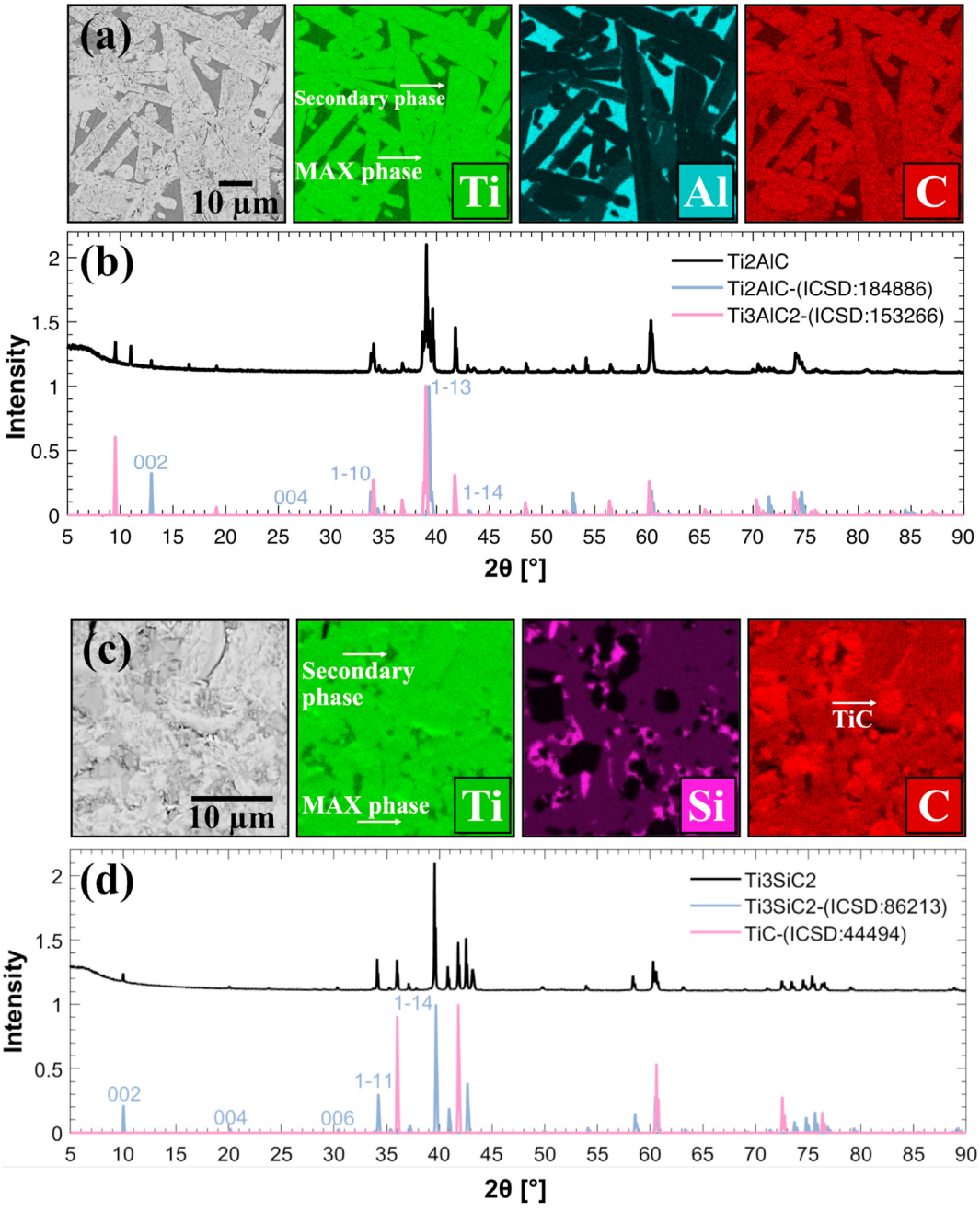

Fig. 1. As-received Ti-based MAX phases (pristine, as-received and unirradiated condition) were investigated within a SEM using BSE and elemental mapping with EDX. Micrographs show the microstructures and elemental maps of the Ti_2AlC and Ti_3SiC_2, (a) and (c), respectively. The elemental quantification is given in Tables 1 and 2 XRD plots in (b) and (d) were obtained from both Ti_2AlC and Ti_3SiC_2, respectively. None of the Ti-based MAX phases samples were phase pure. Note: Labels in the XRD plots are only for the MAX phases of relevance to this work. Additional peaks arise from the presence of unwanted second phases formed during processing.

2. Materials and methods

2.1. Synthesis, provenance, sample preparation, and microscale characterization

The Ti-based MAX phases samples investigated in this work were provided by the company *3-ONE-2* LLC to ORNL. These MAX phases were prepared via the reactive hot pressing technique [34] where pre-reacted powders are poured into a graphite die, then pressure (uni-axial stresses around 40 MPa) and high-temperatures (around of 1500 K) are applied for approximately 4 h. Further details on the bulk synthesis of MAX phases via reactive hot pressing and other methods can be found elsewhere [6,8,35–38].

Two Ti-based MAX phases were investigated: the Ti_3SiC_2 and Ti_2AlC. Prior to electron microscopy characterization, samples were mechanically ground with SiC sheets using grits from 180 to 1600, then subsequently polished with diamond lapping discs down to 1 μm grit size. For the final polishing stage, a compound diamond paste solution was used as abrasive resulting in a mirror-like finish. Scanning electron microscopy (SEM) was used for microscale characterization of the Ti-based MAX phases. A Tescan Mira3 operating at 30 keV was used for general SEM screening and a JEOL JSM-IT300 LV analytical SEM was used for energy dispersive X-ray spectroscopy (EDX) quantification using an Oxford X-Max^N 50 analytical detector with a 50 mm^2 window and with the electron beam energy set to 20 keV. A FEI Apreo SEM was used for SEM-EDX mapping of the Ti-based MAX phases, and for that, the electron beam energy was set to 10 keV to achieve a higher spatial resolution by reducing the interaction volume of the electrons with the sample. Conventional focused ion beam (FIB) was used as the main sample preparation technique for electron microscopy [39] in both *in situ* TEM heavy-ion irradiation experiments and post-irradiation characterization of neutron-irradiated specimens. For FIB milling, a FEI Quanta 3D operating a Ga^+ liquid-metal ion source was used [39].

2.2. X-ray diffraction investigations

X-ray diffraction (XRD) patterns were obtained for both Ti_3SiC_2 and Ti_2AlC MAX phase samples to determine if they were single-phase or non-phase pure samples. In addition, the aim was to determine the identity of secondary phases. Bulk, polycrystalline samples with mirror-like finishes were mounted on a zero background Si crystal plate. XRD measurements were taken using a Bruker AXS D8 advance diffractometer using a Cu-Kα radiation source, Lynxeye XE-T detector in 1D mode, and Bragg-Brentano style geometry. Scans were collected between 5 and 90° 2θ with a step size of 0.02144° 2θ and the detector and source used motorized slits during the measurement. XRD patterns were indexed using available crystallographic data from ICSD (Inorganic Crystal Structure Database).

2.3. In situ TEM annealing

FIB lamellae were annealed within the TEM using a Gatan double-tilt holder with an accuracy of around ±5 K. Samples were annealed from room temperature to 1273 K using a heating rate of 60 K/min^{-1}. For the ion irradiation experiments, the samples were annealed from room temperature to 1008 K using the same heating rate. Prior to the ion irradiation experiments within the TEM, the samples were held at 1008 K for 60 min. After irradiation, samples were cooled down to room temperature by switching off the heating holder, resulting in a cooling rate of approximately 300 K/min^{-1}. Images were extracted from the video during the heating ramp, at 1273 K and after cooling to room temperature.

Table 1
Pristine Ti_2AlC elemental composition as measured by SEM-EDX (error is 5% of each value).

Element	Measured [wt.%]	Expected [wt.%]	Measured [at.%]	Expected [at.%]
Ti	70.3	71.0	45.6	50.0
Al	15.6	20.0	18.0	25.0
C	14.0	9.0	36.3	25.0

2.4. Neutron irradiation at the HFIR

For the neutron irradiations, both bulk Ti-based MAX phases were irradiated at the ORNL's HFIR up to fluences of 2×10^{21} and 1×10^{22} n/cm^{-2}. These fluences correspond to a dose of 2 and 10 dpa, respectively. The irradiations at the HFIR were carried out at a temperature of 1273 K. Samples were safely stored in a cooling pond after irradiation in order to wait for activity reduction. ORNL's low activation materials development and analysis laboratory was used to prepare and characterize specimens post-irradiation, using SEM, FIB, and TEM.

2.5. Heavy ion irradiations at the MIAMI-2 facility

Parallel to the neutron irradiations at HFIR, a study on the heavy-ion irradiation response *in situ* within a TEM at the MIAMI-2 facility at the University of Huddersfield (UK) [40] was carried out using electron-transparent pristine (unirradiated) Ti_3SiC_2 and Ti_2AlC samples. The ion beam energy was set to 700 keV using Kr^{+2} ions, thus matching the average primary knock-on atom (PKA) energy of the Ti-based MAX phases constituents generated by neutron irradiation in a materials test reactor like HFIR. It should be noted that the ion irradiations were conducted at a lower temperature than that of the HFIR irradiations, *i.e.* 1008 K. The reasons for the different irradiation temperatures will be discussed in Section 3.2. Annealing and irradiations at 1008 K were carried out using a Gatan double-tilt heating holder. Further details on the heavy-ion irradiation conditions and dose achieved in this work can be found in the supplemental materials file.

For comparison with the heavy-ion irradiation of MAX phases, α-Ti and α-Al elemental metals were irradiated under identical ion beam conditions, although the irradiation temperatures were set instead to 1143 and 558 K, respectively, for Ti and Al. For both Ti-based MAX phases and elemental metals ion irradiated in this work, the irradiation temperatures were chosen to match the homologous temperature of $0.60T_m$. This comparison serves to elucidate different mechanisms of radiation damage and defect transport between metals and MAX phases.

3. Results and discussion

3.1. Electron microscopy and XRD characterizations of pristine specimens

Microstructures and elemental mapping of the pristine (unirradiated) Ti-based MAX phases are presented in the SEM micrographs in Fig. 1(a) and (c). Both Ti_2AlC and Ti_3SiC_2 grains show light-

Table 2
Pristine Ti_3SiC_2 elemental composition as measured by SEM-EDX (error is 5% of each value).

Element	Measured [wt.%]	Expected [wt.%]	Measured [at.%]	Expected [at.%]
Ti	69.8	73.5	43.1	50.0
Si	12.4	14.3	13.1	17.0
C	17.8	12.2	43.8	33.0

gray contrast when viewed using the backscattered electron (BSE) detector within the SEM. The MAX phase grains are also of distinct morphology, resembling lath-shaped grains preferentially elongated in one direction. The presence of both MAX phases as the light-gray areas was confirmed using SEM-EDX as shown in the elemental maps acquired from both specimens. The elemental composition quantification of the MAX phases areas using the Cliff-Lorimer method are shown in Tables 1 and 2. The ratios between Ti/Al and Ti/Si are approximately 2:1 and 3:1 within an error of ±3% and ±10%, respectively. The use of SEM-EDX to characterize C-containing phases precludes correct quantification of this element, thus the measured compositions may slightly deviate from expected stoichiometries. This is due to carbonaceous contamination in either the samples' surfaces or the window of the detector attenuating the low energy X-ray signals prohibiting the accurate quantification of low Z elements such as C. The SEM thus poses inherent difficulties to correctly quantify C. The ratio method presented above was recently acknowledged as a possible method to characterize MAX phases containing C [41]. In our measurements, the overestimation of C in quantification is around 12%.

By analyzing contrast differences in Fig. 1(a) and (c), the presence of secondary phases in both Ti_2AlC and Ti_3SiC_2 samples was revealed: when viewed using the BSE detector, which is sensitive to the average Z of phases, such secondary phases show dark-gray contrast as opposed to the light-gray contrast arising from MAX phases. In Fig. 1, the SEM-EDX elemental mapping shows both Ti-based MAX phases and these secondary phases within the mesoscale: the secondary phase present in the Ti_2AlC sample is Al-rich whereas for the Ti_3SiC_2 sample, the secondary phase is Si-rich. The depletion of C in both Al- and Si-rich secondary phases suggests that these may be Ti aluminides and Ti silicides. It is worth emphasizing that in the Ti_3SiC_2, the binary Ti carbide has been also detected via SEM-EDX mapping as shown in the C map in Fig. 1(c).

In order to evaluate the presence of MAX phases in the samples as-received, a series of XRD measurements were performed and the results are shown in Fig. 1(b) and (d), respectively, for the Ti_2AlC and Ti_3SiC_2. The results agree with the SEM investigations presented in Section 3.1, and specifically, these show that both stoichiometric Ti-based MAX phases are present in the specimens, *i.e.* the 2-1-1 phase within the Ti—Al—C system and the 3-1-2 phase within the Ti—Si—C system. It is worth emphasizing that the basal reflections were identified for both specimens at lower angles, which unequivocally demonstrates the hexagonal-compact nature of these phases.

Secondary phases were also observed in the XRD data for both specimens. In the Ti—Al—C system, a 3-1-2 MAX phase was detected, Ti_3AlC_2, in which the intensities of the 3-1-2 phase are lower than that of the Ti_2AlC phase, suggesting that the latter is the major phase in the sample. In the Ti—Si—C system, a secondary phase of binary Ti carbide was detected that was again lower than that of the Ti_3SiC_2, indicating that the Ti_3SiC_2 is the primary phase present. The Ti carbide was also detected in the SEM-EDX mapping presented in Fig. 1(c). While preferential orientation (*i.e.* texture) can impair the proper detection of the Ti aluminides and Ti silicides secondary

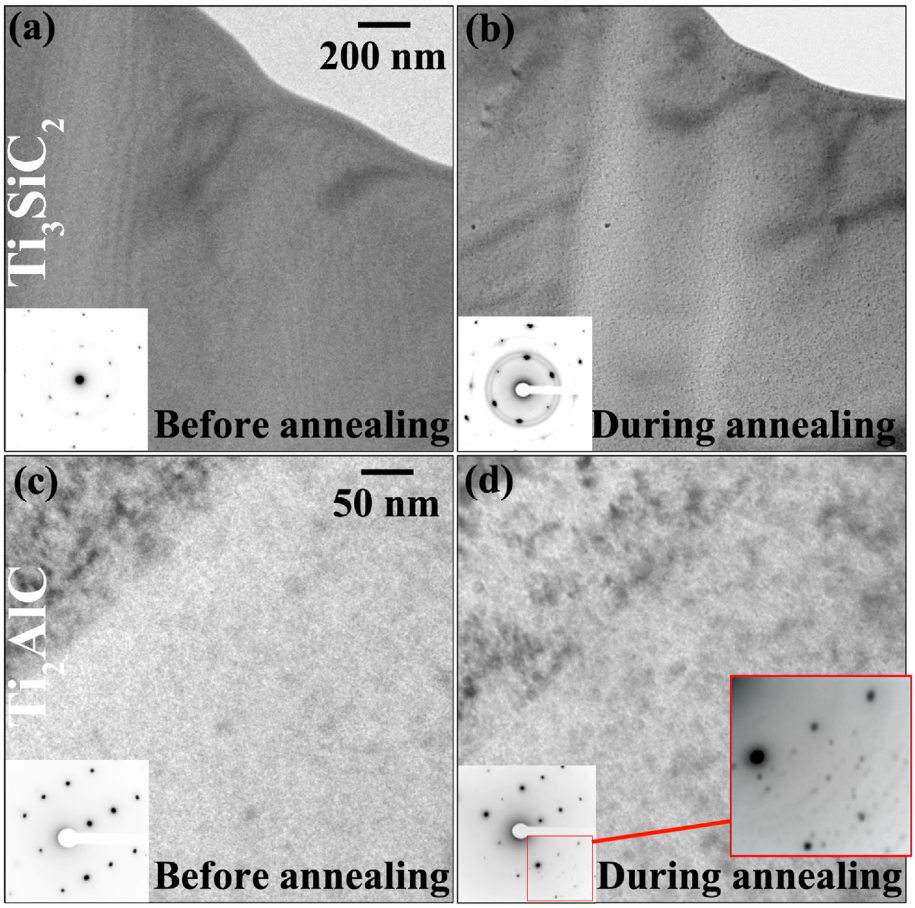

Fig. 2. *In situ* TEM annealing response of the Ti_3SiC_2 (a) before and (b) during annealing at 1073 K and of the Ti_2AlC (c) before and (d) during annealing at 1273 K. Debye-Scherrer rings are observed in the diffraction patterns for the Ti_3SiC_2 during annealing whereas the SAED for Ti_2AlC reveals the formation of polycrystalline features. Note: the scale bar in (a) also applies to (b) and the scale bar in (c) also applies to (d).

phases, the results obtained with XRD support the conclusions observed from the SEM-EDX results presented above: both SEM-EDX and XRD data indicate that the unirradiated Ti-based MAX phase materials as-received are not phase pure.

Hence, we have used FIB to lift-out TEM samples from the 'pure' MAX phase grains at the microscale for our irradiation studies. At the nanoscale, undesired second phases may also be present within the MAX phase microstructure, as previously observed for the Ti_3SiC_2 in the TEM [21,42] but that were not so far observed in the Ti_2AlC. Although not phase pure at the microscale, the samples studied in this work were found to be free of other impurities.

3.2. Electron microscopy characterization of specimens under in situ TEM annealing

In situ TEM annealing was carried out to investigate the thermodynamic stability of both MAX phases and to evaluate whether Ti-based MAX phases are stable compounds under high heating rates (60 K/min^{-1}) and at high-temperatures (1273 K), tested within the environment of a TEM (*i.e.* under vacuum and a thin electron-transparent film). Pristine specimens for the *in situ* TEM annealing experiments were lifted-out from the MAX phase regions of the bulk specimens as discussed in Section 3.1 that were observed as the stoichiometric 3-1-2 and 2-1-1 MAX phases. Protective layers—typically C or Pt—were not used in the FIB-based preparation of samples, as these elements are known and have been observed to diffuse across the surface of the thin foil specimens at moderate temperatures below those of interest here, severely impeding microstructural characterization. This may result in some Ga contamination due to the use of the FIB, but this is not expected to alter the high temperature behavior significantly.

At room temperature, both Ti-based MAX phases were observed to be free of defects as seen in the bright-field TEM (BFTEM) micrographs presented in Fig. 2(a) and (b), for the Ti_3SiC_2 and Ti_2AlC MAX phases, respectively. The selected-area electron diffraction (SAED) pattern inset of these micrographs also show the MAX phases are phase pure after FIB: neither secondary phases nor amorphous regions were observed in the samples. Immediately following high temperature annealing, small rounded precipitates were observed to form within these microstructures as can be noted in the BFTEM micrographs in Fig. 2(b) and (d). The precipitation was also confirmed by analyzing the SAED patterns: the presence of Debye-Scherrer rings—indicative of the amorphous phase—is revealed in the Ti_3SiC_2 (inset in Fig. 2(b)) whereas similar matrix phase decomposition manifested without the noticeable formation of Debye-Scherrer rings in the Ti_2AlC, in which extra diffraction-spots were observed in the SAED (inset in Fig. 2(d)). This indicates amorphous decomposition in Ti_3SiC_2 and crystalline phase decomposition in Ti_2AlC. It is worth emphasizing that during several *in situ* TEM annealing experiments conducted, the MAX

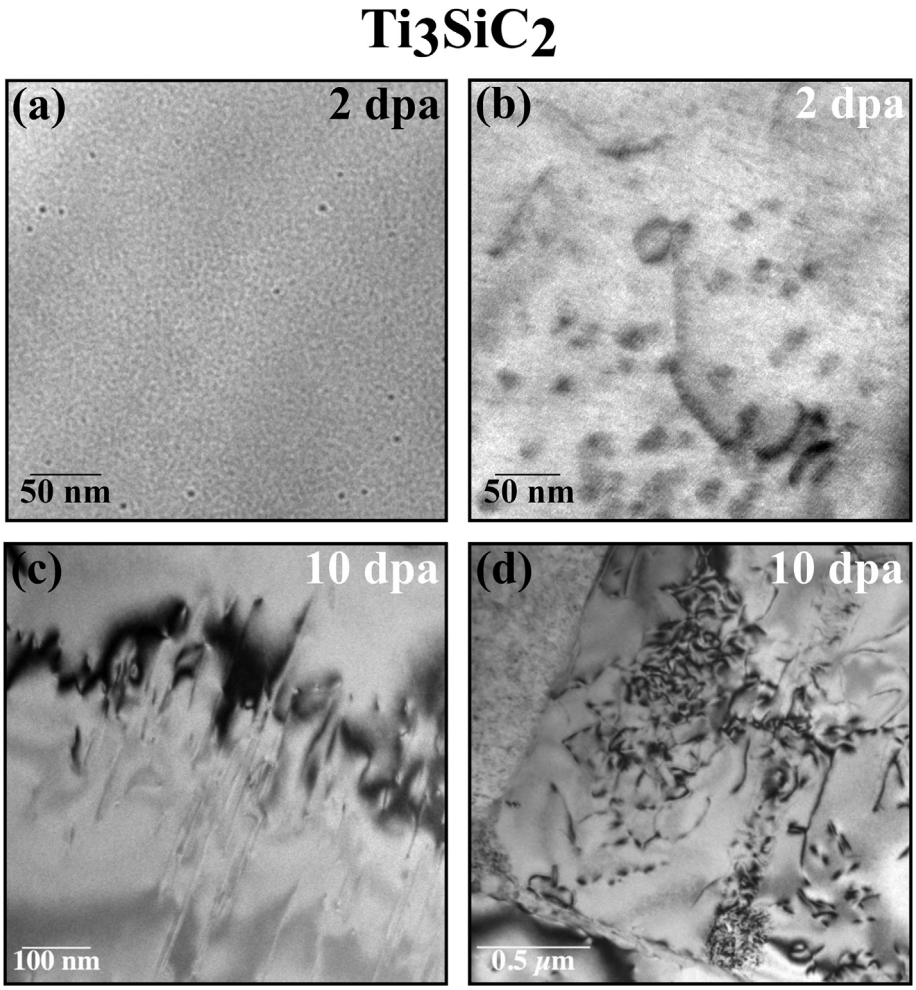

Fig. 3. TEM micrographs of neutron-irradiated Ti_3SiC_2 showing the presence of (a) nanometer-sized voids (overfocus of 2 μm), (b) dislocation loops, (c) transgranular dislocation lines, and (d) disordered dislocation network.

phase decomposition effect started (only) at around 973 K for the Ti_3SiC_2 and at 1173 K for the Ti_2AlC.

The thin film effect must also be considered as the thermal annealing was conducted on TEM thin foils and not bulk specimens. Heating MAX phases within the TEM results in an increase of the concentration of vacancies in equilibrium, thus activating solid-state diffusion. In an electron-transparent specimen, additional factors may govern the precipitation of secondary phases during *in situ* TEM annealing experiments: (i) the excess of mobile defects such as equilibrium vacancies, (ii) their agglomeration, and (iii) the presence of free surfaces of thin specimens (tens of nm). These factors, or their combination, contribute to an increase of the Gibbs potential of the heterogeneous equilibrium within the system [43], thus phase instabilities and decomposition may manifest if the thermodynamic conditions are favorable.

In the specific case of Ti_3SiC_2 and Ti_2AlC, phase instabilities upon heating will be driven by the competition between the MAX matrices and the binary transition metal carbides ('AX' and/or 'MX') [44,45]. The excess of equilibrium vacancies at high-temperatures will increase the kinetics of solid-state diffusion, as manifested by an increase of the mobility rates of the atomic constituents. Given the presence of free surfaces in the electron-transparent lamellae, which can act as preferential sink sites for defects, an increase in diffusion rates may lead to a heterogeneous nucleation process of precipitation. Density functional theory (DFT) and *ab initio* methods have been used to study the formation, accumulation, and migration of defects in model Ti-based MAX phases [26], the results of which demonstrated that C interstitial atoms can be formed easily within these Ti-based MAX phases, and their recombination with vacancies was far more energetically unfavorable which may lead to significant accumulation of C atoms within the Si layers. It was also determined that such C interstitials may bind with Ti and Si, *"(…) in a manner very similar to the binary carbides SiC and TiC"* [26]. Considering the computational results obtained by Middleburgh et al. [26], the phase decomposition observed to take place in the Ti-based MAX phases herein investigated is a precipitation effect arising from the fast diffusion of C interstitials within the A layers, combining with Ti and Si, promoting binary carbides nucleation. An analytical characterization of the Ti_3SiC_2 specimen after *in situ* TEM annealing is presented in the supplemental information file.

3.3. Neutron irradiations in the HFIR

The research presented in this section complements a large research study on the effects of neutron irradiation on select Ti-based MAX phases [21]. BFTEM micrographs of the Ti_3SiC_2 MAX phase irradiated with neutrons to 2 and 10 dpa are shown in Fig. 3. Some irradiation effects within the microstructure of this material are clearly visible. For example, at 2 dpa, Fig. 3(a) shows the presence of voids/cavities randomly distributed within the grain and with diameter of around 3–7 nm whereas Fig. 3(b) shows the presence of irradiation-induced dislocation lines and loops. On

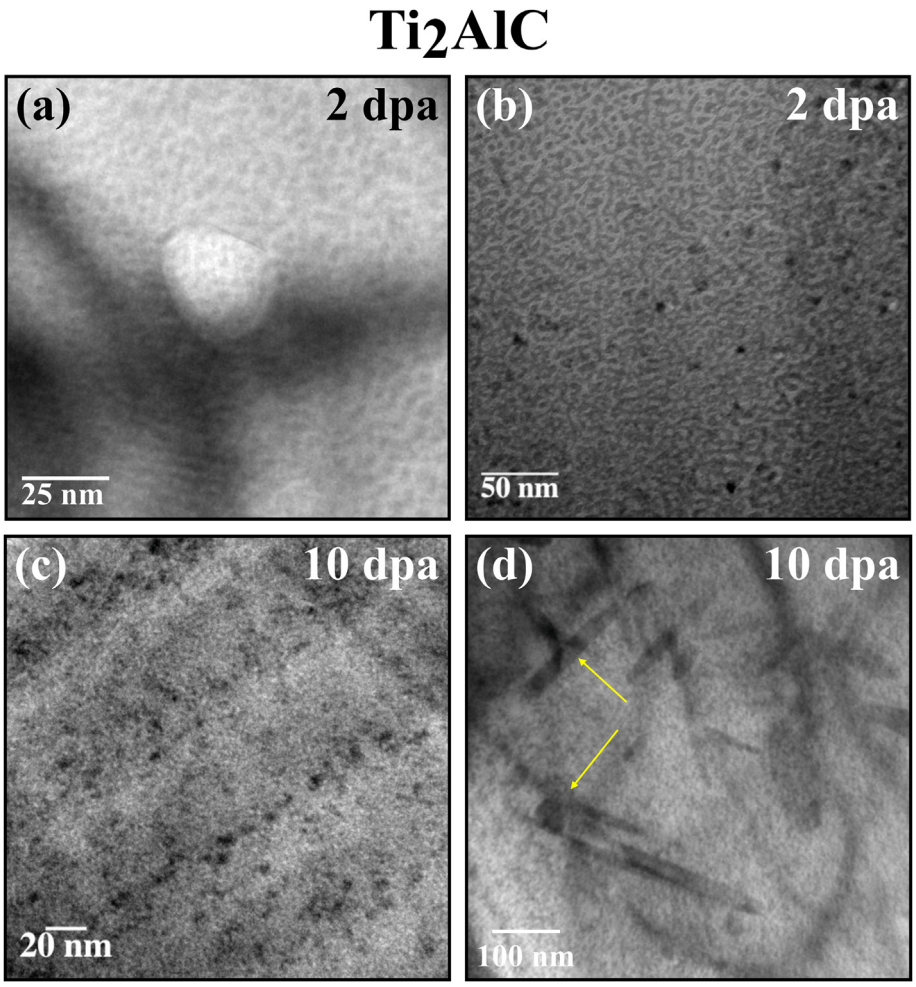

Fig. 4. TEM micrographs of neutron-irradiated Ti_2AlC showing the presence of (a) large voids (underfocus of 2 μm), (b) black-spots and degraded matrix phase, (c) nanometer-sized voids (underfocus of 1 μm) and black-spots, and (d) irradiation-induced precipitation pointed by yellow arrows.

increasing the dose to 10 dpa, long transgranular dislocation lines are observed to form within grains as shown in Fig. 3(c), and the formation of a disordered dislocation network is noted at the highest dose as depicted in Fig. 3(d).

Similarly, Fig. 4 shows typical irradiation effects observed under BFTEM conditions in the Ti_2AlC MAX phase with neutron doses to 2 and 10 dpa. At 2 dpa, the under focused BFTEM micrograph in Fig. 4(a) exhibits small and large voids/cavities close to a grain boundary. Black-spot damage is observed throughout the matrix phase as shown in Fig. 4(b) at 2 dpa and 4(c) at 10 dpa, the latter accompanying the presence of small voids. At 10 dpa, the formation of plate-like and spherical precipitates of an unknown phase was detected in the Ti_2AlC MAX phase matrix.

As a general trend on the neutron irradiation effects on these two Ti-based MAX phases, together with previous results published on these samples [21], the following list summarizes the observations arising from the detailed electron microscopy investigations:

- Black-spots and dislocation loops are observed to form at 2 and 10 dpa in both Ti-based MAX phases, but disordered dislocation networks were observed at 10 dpa for the Ti_3SiC_2. The nature of such dislocations were investigated in previous work [21] and were found to be constrained within the basal planes due to the high c/a ratio of these materials, forming $<a>$ loops.
- Small cavities were observed in both Ti-based MAX phases, but large cavities were noticeable only in the Ti_2AlC.
- Irradiation-induced precipitation at 10 dpa was observed to occur for the Ti_2AlC, with previous work reporting similar irradiation-induced precipitates at 10 dpa for Ti_3SiC_2 [21].

From the results on neutron irradiation of Ti-based MAX phases presented here, combined with previous literature published on this topic [18–21], it is worth emphasizing that radiation damage does develop within the microstructure of these new nanolayered materials. Previous neutron irradiations were performed to a total dose of 3 dpa (which is considered a very low dose for materials for new reactor concepts, which are expected to receive doses of 200–500 dpa) displayed evidence of radiation damage [18–20]. Here, it is shown that for doses up to 10 dpa at high temperatures, radiation damage results in the formation of precipitates, questioning the thermodynamic stability of these materials under neutron irradiation at high temperatures.

MAX phases have already been proposed for use in the next generation of nuclear reactors operating at high-temperatures as a fuel cladding material [46]. Molten-salt reactors may also provide a potential application of MAX phases. These reactors operate in the temperature range of 973–1273 K and up to doses of 200 dpa with a thermal neutron spectrum [47]. However, the data on neutron-irradiated Ti-based MAX phases—although limited—suggests these materials can experience thermodynamic phase instabilities leading to the formation of undesired secondary phases that may significantly alter their initial properties. Additionally, the current

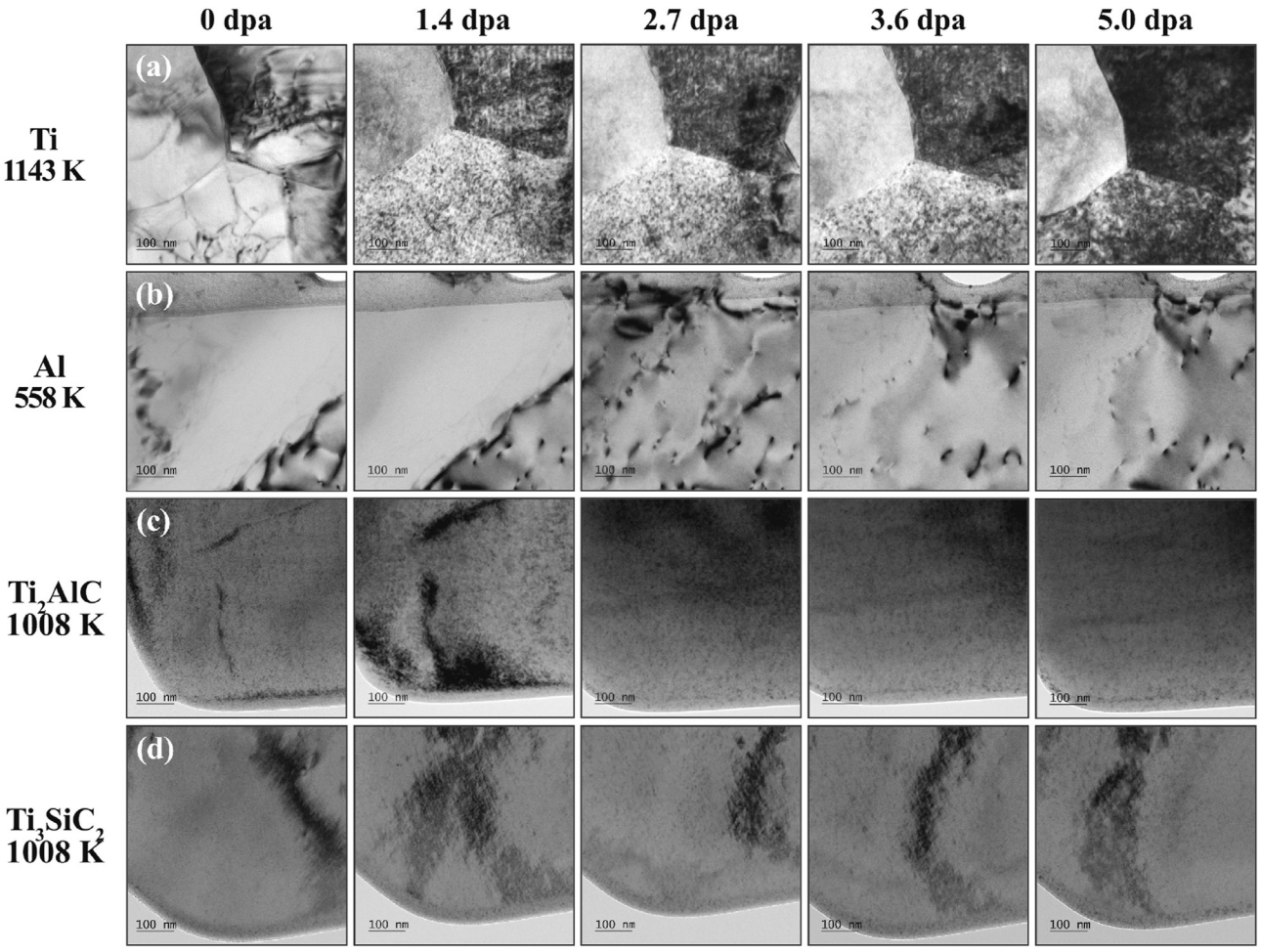

Fig. 5. *In situ* TEM heavy ion irradiation of the pure Ti and Al metals and the Ti-based MAX phases (see figure 5). Note: video time length is up to 5 dpa.

literature on the neutron irradiation response [18–21] suggests that both displacement damage build-up and accumulation, including the formation of cavities at relatively low doses, may be an indication that their envisaged radiation tolerance demands further investigations as the current framework points towards these materials not being suitable for application in nuclear reactors operating at high-temperatures.

3.4. Heavy-ion irradiations with in situ TEM

As discussed in Section 3.2, the *in situ* TEM annealing of both Ti-based MAX phases within the TEM up to temperatures approximately above 1000 K resulted in the formation of fine precipitates, which were found to be detrimental for analyzing their response to *in situ* TEM heavy ion irradiation. As such, the irradiation temperature for the MAX phases in this work was set to 1008 K, which although does not reproduce directly the neutron irradiations at HFIR (carried out at 1273 K), it is the same temperature used for previous neutron irradiation studies on the same MAX phases [20]. In addition, as this chosen temperature is above the expected vacancy mobility for Ti-based MAX phases [26] it is not anticipated that there will be a significant variation in microstructural evolution.

Regarding the *in situ* TEM heavy ion irradiation experimental setup, an ion beam consisting of 700 keV Kr^{+2} was chosen. This ion species and energy simulates the average PKA energies caused by neutrons within nuclear fusion reactor spectra as calculated by Gilbert et al. using the FISPACT code [48] and the elements that form both Ti-based MAX phases herein under investigation. These irradiation conditions (depicted in Fig. 1) may result in a maximum Kr implantation level of around 1%. In order to differentiate the mechanisms of radiation damage in both Ti-based MAX phases, elemental metal α-Ti and α-Al specimens were also irradiated at a temperature corresponding to the homologous temperature of $0.6T_m$. The irradiation temperature of the MAX phase specimens was also $0.6T_m$.

It is worth emphasizing that the *in situ* TEM heavy ion irradiation experiments were performed with the Ti-based MAX phase samples in multi-beam conditions. In this way, if displacement damage occurs, they will be visible under BFTEM conditions.

Results of the *in situ* TEM heavy ion irradiations to 5 dpa for α-Ti, α-Al, T_2AlC, and Ti_3SiC_2 are shown in Fig. 5. Radiation damage in the form of black-spots was observed in metallic Ti at doses as low as 1.4 dpa and significant accumulation of such type of damage was observed within Ti grains at a dose of 5 dpa. Conversely, the dislocation loops were observed to form as a result of irradiation in Al at doses around of 1.4 dpa and became mobile under irradiation, in contrast to the irradiations performed on Ti where accumulation has been recorded. In addition to displacement damage, nanometer-sized cavities were observed to form in both Ti and Al as shown in Fig. 6.

The *in situ* TEM evolution of both MAX phases subjected to heavy ion irradiation are also shown in Fig. 5. Unlike the ion irradiation experiments in the elemental metals, radiation damage effects were not detected in either Ti-based MAX phases up to a dose of 5 dpa under the studied conditions. The black-spot-like contrast observed in both MAX phases are due to the effects of thermal annealing of the TEM lamellae as shown in Section 3.2 arising as a result of matrix phase decomposition: which is still quite significant when the samples were held at 1008 K for extended periods. It is worth emphasizing that these black-spots are present in the MAX phases before irradiation, as shown in Fig. 5 at 0 dpa. Both MAX phases were held at 1008 K for 30 min prior irradiation. Irradiation defects such as dislocation loops and cavities were not observed to form in the Ti-based MAX phases. In addition, by monitoring the diffraction pattern

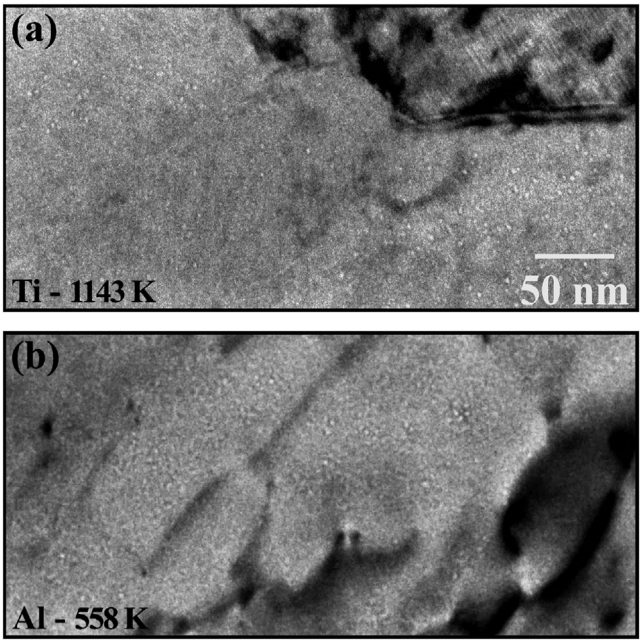

Fig. 6. Nanometer-sized voids identified in the elemental metal specimens after irradiation: pure (a) Ti and (b) Al. Similar voids were not observed in the Ti-based MAX phases under heavy-ion irradiation up to 5 dpa at 1008 K. Note: both micrographs were taken with a defocus level of ≈ 1000 nm.

of both MAX phases before and after irradiation up to 5 dpa (Fig. 7), no amorphization was observed under irradiation. It is worth noting that Debye-Scherrer rings are present in the diffraction patterns of the Ti_3SiC_2 before irradiation, demonstrating these features are present in the non-irradiated condition and are neither formed nor modified as a result of irradiation.

Here, the *in situ* TEM heavy ion irradiation results present an apparent contradiction with the neutron post-irradiation observations as the ion beam setup was chosen to reproduce the average PKA energy experienced by Ti-based MAX phases when in a nuclear fusion reactor. Conversely, radiation damage was indeed observed in the metal counterparts. A question that remains to be answered is: why no apparent radiation damage was observed under the studied ion irradiation conditions on the Ti-based MAX phases?

To address such a question, we resort to previous research examining electronic energy dissipation in metals, multicomponent metallic alloys and ceramics under ion irradiation to provide some insights [49]. In some circumstances depending on the target species and irradiation depth, ion irradiation leads to annealing of both pre-existing and irradiation-induced crystalline defects in materials that is strongly dependent on the competing ratio between the nuclear and electronic energy loss mechanisms. This effect is known as ionization-induced annealing (IIA) [49]. In general, what dictates whether IIA is likely to occur is the energy and species of the ion beam: this effect has been reported to be predominant in covalent ceramic materials when the electronic energy loss mechanism dominates the stopping power [50]. For example, in the case of SiC, the electronic energy was linked to IIA to prevent amorphization of the material under irradiation [50]. IIA can be viewed as a competing radiation effect to damage due to pure atomic collisions in solids, *i.e.* nuclear stopping. While in the latter, damage energy is dissipated within the lattice in the form of ballistic collisions generating atomic displacements, in the former, electronic energy is dissipated promoting heating (and also thermal spikes [51]) via ionization, resulting in defect annealing within the material. Bond breaking and rearrangement of bonding are also

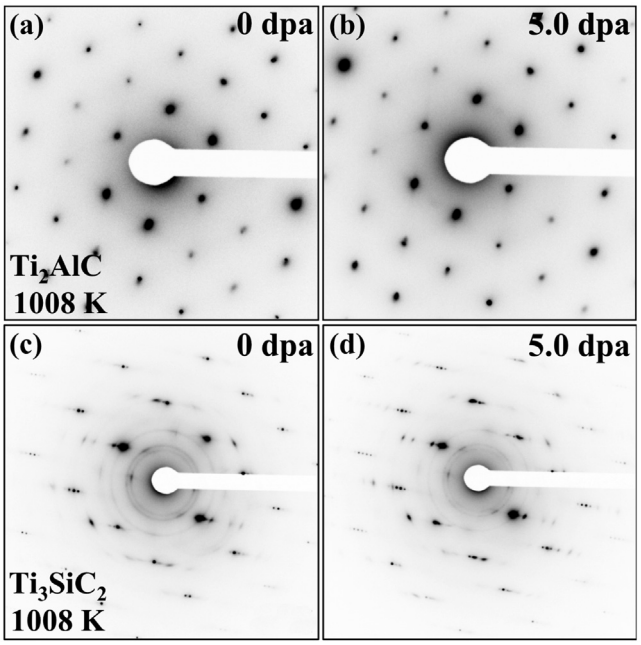

Fig. 7. Diffraction patterns taken at 0 dpa after annealing (a), (c) and 5 dpa after irradiation (b), (d) with 700 keV Kr^2 ions at 1008 K indicate that both Ti_2AlC and Ti_3SiC_2 MAX phases have not experienced any amorphization under the studied conditions. Note: the Debye-Scherrer rings present in the Ti_3SiC_2 diffraction patterns taken at 0 dpa are due to the phase decomposition induced solely by thermal annealing prior irradiation (see Section 3.2) and do not appear to be modified by irradiation.

secondary effects induced by electronic energy deposition in ceramics.

Aimed at determining whether the electronic stopping may influence the results observed in Fig. 5, a series of calculations using pySRIM was performed. This set of Python codes coupled with SRIM comprise a unique platform to estimate energy deposition from nuclear and electronic stopping powers in materials [50,52]. The results of the pySRIM analysis in both Ti-based MAX phases are shown in Fig. 8. The plots of deposited energy per total ions in both Ti_3SiC_2 and Ti_2AlC show that the total damage energy (arising from pure ballistic collisions either from ions or recoils) level is slightly lower than the total ionization considering both ions and recoils. These calculations show that despite the fact that the ion-target collision profiles are similar for both materials (see Fig. 1), the ion irradiation conditions chosen in this work, *i.e.* 700 keV Kr^+ ions, although intended to simulate the PKA energies caused by the neutron spectra within a nuclear fission reactor, can generate a large yield for electronic energy dissipation in a form of ionization. This scenario indicates that IIA is prone to occur in the Ti-based MAX phases under the conditions herein investigated, thus possibly mitigating the appearance of radiation damage in these materials. This evaluation using pySRIM suggests that there is a synergistic coupling between damage energy arising from nuclear ballistic collisions, generating displacements, with the concurrent electronic energy deposition, promoting IIA. It is worth emphasizing that in terms of chemical bonding, MAX phases are neither considered pure metallic or ionic nor covalent, but rather a mixture of these three types of chemical bonding [53]. Therefore, the phenomenon of IIA should be further investigated in materials that present mixed chemical bonding character such as MAX phases.

A second fact that must be discussed using the results obtained with the *in situ* TEM heavy ion irradiation experiments of MAX phases and metals is on point defect energetics. By using DFT calculations, Middleburgh et al. estimated the formation energies for Frenkel pairs in both Ti_3SiC_2 and Ti_3AlC_2 (the latter is not investigated in the present study) [26]. For the Ti_3SiC_2, these Frenkel pair formations energies were 6.46, 2.59, and 2.93 eV, respectively, for Ti, Si, and C. By comparing data available in literature for Frenkel pair formation energy in α-Al and α-Ti, the values are 3.67 and 3.85 eV, respectively [53–59]. It is generally accepted that the higher the energy to form a Frenkel pair, fewer point defects will be formed under irradiation. From the DFT results discussed above, it is harder to displace Ti to form Frenkel pairs within MAX phases M-layers than the metallic α-Al and α-Ti, although the energy required to displace Si and C atoms in MAX phases A- and X-layers is lower than the elemental metals. However, as previously shown [26], a trend for more efficient recombination of defects within the MAX phases A-layers is prone to occur at low to moderate temperatures, resulting in a 'self-healing' effect at these layers under irradiation. Similar behavior is not observed in the elemental metals. These considerations arising from DFT calculations indicate on a trend where it is harder to produce Frenkel pairs in MAX phases when compared with the metals. In addition, the nanolayered nature of MAX phases spatially constrains diffusion, thus enhancing recombination. In combination with the aforementioned IIA phenomenon combined with the tendency for the recombination of defects formed as per irradiation via electronic energy deposition and ionization, defect energetics may play a role in the absence of radiation-induced defects in the MAX phases microstructures observed. Nevertheless, the direct *in situ* TEM heavy-ion irradiation comparison between the elemental metal constituents and the MAX phases also suggests that in metals, the mechanisms of radiation transport, diffusion, and generation of defects are completely different than the MAX phases, which requires further research to understand the defect formation and recovery in these unique nanolayered ceramics in which preferential defect recombination in 2D planes may be dominant.

Finally, the role of dose rate in the irradiation of the Ti-based MAX phases must be considered. In this work, the neutron irradiations carried out in the HFIR were completed over years[g] whereas the *in situ* TEM ion irradiation presented was performed in a matter of hours. This creates a scenario where the ion dose rate is orders of magnitude higher than the neutron dose rate. Available literature on dose rate effects is rich for structural nuclear materials [60–64], such as steels, but non-existent for MAX phases. Although in steels the effects of dose rate on the microstructural evolution under irradiation is a well reported phenomenon, further studies are required to determine the exact causes and consequences [64]. The current understanding is that low dose neutron irradiation does not induce ballistic mixing, leading to the 'healing' of the majority of point defects induced by irradiation (*i.e.* higher recombination rates) [63]. In this case, defect cascade generation is slower, thus limiting the ability of displacement damage (such as loops) to form with higher densities, but promoting their ability to grow within the interior of the grain as not many interactions takes place [61]. Conversely, the high dose rate characteristic of ion irradiation promotes ballistic mixing due to insufficient time for point defect recovery (*i.e.* lower recombination rates) [63], leading to the development and significant accumulation of damage throughout the irradiated microstructure [61]. In the latter case, the areal density of defects is high and the size of the defects is smaller than in the neutron irradiation case. Both solid-state diffusion and precipitation are also believed to be faster in steels subjected to higher

[g] HFIR's dose rate is material specific but in general, a dose rate of is 6 dpa/year^{-1} is reported for metallic alloys of relevance to the nuclear industry. Source: Nuclear Energy Advisory Committee, Assessment of Missions and Requirements for a new U.S. Test Reactor, 2017.

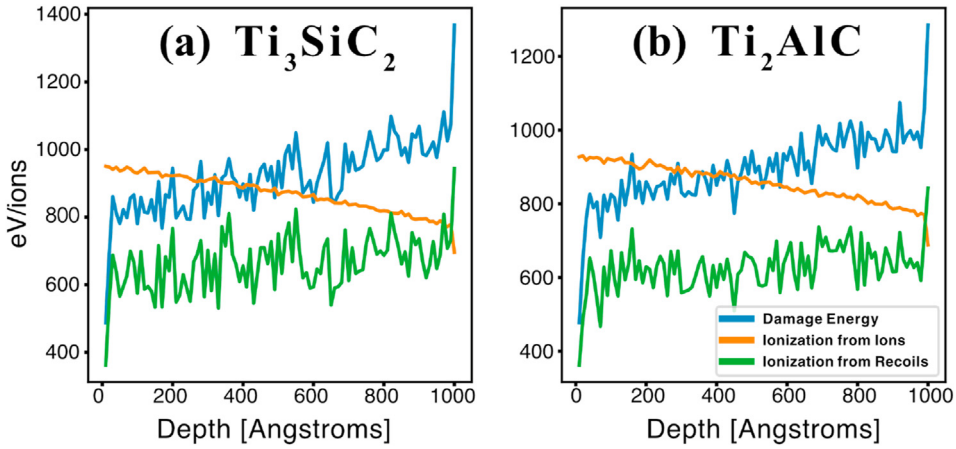

Fig. 8. Analysis using pySRIM [50,52] on the *in situ* TEM heavy ion irradiation conditions used in this work to study the radiation effects in both Ti-based MAX phases: (a) Ti_3SiC_2 and (b) Ti_2AlC. The pySRIM analysis was performed considering a TEM lamella with thickness set to 100 nm. The plots in the figure show the energy deposited into the lattice due to damage (nuclear stopping, blue curves) and ionization from ions and recoils (electronic stopping, orange, and green curves). These plots are normalized by the total number of ions calculated (20 k).

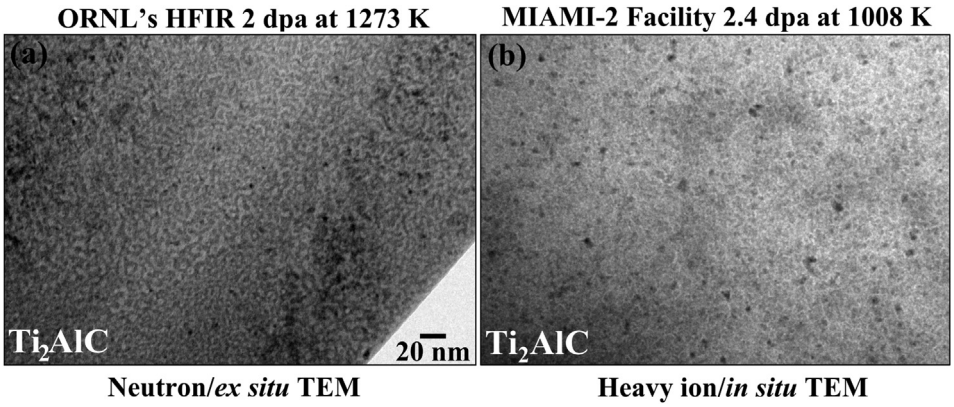

Fig. 9. A comparison between (a) neutron irradiation with (b) ion irradiation indicates that the heavy-ion irradiated damage microstructure of the T_2AlC at 2.4 dpa (b) and 1008 K could be reproduced in agreement with the damage microstructure from neutrons at around 2 dpa at 1273 K (a). It is worth emphasizing that such agreement was noted only in a single experiment (out of 17 identical ion irradiation runs at the MIAMI-2 facility). Note: both micrographs were taken under same magnification, thus the scale bar in (a) also applies to (b).

dose rates, but smaller precipitates induced by irradiation are observed in ion irradiated specimens than neutron-irradiated ones [62].

Extended radiation-induced defects were indeed observed in the MAX phases using neutron irradiation. Large precipitates and large dislocations, for example, were observed as shown in Figs. 3 and 4. But in the ion irradiation case, no radiation damage at all was observed. This suggests that, coupled with IIA effects, higher dose rates can significantly promote higher recombination rates within the microstructure of Ti-based MAX phases, leading to a self-healing effect [26] and experimentally observed in several other ion irradiation cases of MAX phases [22,28,32]. Further studies are needed to define the dose rate regimes by which radiation damage may manifest within the microstructure of MAX phases, either by neutron or ion irradiation.

Despite the evidence suggesting that a direct heavy-ion and neutron irradiation effects comparison in Ti-based MAX phases was not possible under the chosen experimental conditions, in a single experiment (out of 17 heavy-ion experiments performed with these MAX phases), the microstructure of the Ti_2AlC irradiated at 1008 K up to a dose of 2.8 dpa was found to be very similar with the neutron-irradiated material up to a dose of 2.0 dpa at 1273 K. This isolated result is shown in Fig. 9. Black-spots are observed in both materials with evidence that the matrix phase of the Ti_2AlC has degraded, although a more detailed characterization of such microstructures using the analytical TEM was not performed. It is worth emphasizing that such black-spots could be a result of the MAX phase exposure to high temperatures, as discussed in Section 3.2, and not properly due to irradiation.

4. Conclusions

A detailed study on the stability of Ti-based MAX phases when exposed to high-temperatures, neutron irradiation, and heavy-ion irradiation is presented. The as-received MAX phase samples were not phase pure at the mesoscale, as assessed via SEM-EDX and XRD; however, for the TEM work that followed, electron-transparent samples were lifted-out using FIB from the stoichiometric MAX phase regions.

When exposed to high-temperatures, evidence suggests that the matrix phase of both T_2AlC and T_3SiC_2 experienced phase instabilities resulting in the formation of fine precipitates. The precipitation was observed *in situ* within the TEM to initiate at a temperature around 1073 K, and the microstructure comprising

both matrices and precipitates was stable up to 1273 K. The active role of such precipitates in the radiation response of both Ti-based MAX phases is unknown, but in a recent study, the presence of amorphous nanoprecipitates within the microstructure of the Cr_2AlC MAX phase was related with a higher radiation resistance as they can act as sinks for irradiation-induced defects [32].

Different types of radiation damage are observed to occur in both Ti-based MAX phases when under neutron irradiation at 2 and 10 dpa, such as the formation of black-spots, dislocation loops and disordered networks of dislocations, cavities or voids and also radiation-induced precipitation. These neutron irradiation data agrees with previously published data on the same materials irradiated at lower temperatures and lower doses [18–20] and also with previous research published by our group [21].

Under heavy-ion irradiation *in situ* within a TEM, surprisingly, radiation effects were not detected in both Ti-based MAX phases microstructures. The "'high' resistance of these materials to ion irradiation can be attributed to the hypothesis that ionization caused by ions and recoils using the chosen irradiation conditions (700 keV Kr^2 ions at 1008 K) is prone to induce annealing of crystalline defects as this electronic energy deposition into the lattice can cause local heating. Therefore, the coupling phenomena between nuclear and electronic energies depositions suggests that the manifestation of radiation damage within these Ti-based MAX phases is significantly suppressed or mitigated. A direct comparison between pure Ti and Al under identical irradiation conditions was made and indicates that the mechanisms of formation and diffusion of crystalline defects are completely different in the Ti-based MAX phases, a fact that motivates further works in this particular topic. Under the chosen experimental conditions, a comparison between neutron and ion irradiation effects was not possible.

Given the facts and evidence presented, a question remains to be answered: can Ti-based MAX phases be considered for applications in future nuclear reactors operating at high-temperatures and sustaining high dose levels? This present work in combination with the available (but so far limited) literature on these materials suggests that such Ti-based MAX phases cannot be considered stable materials when exposed to either high-temperatures or low-dose neutron-irradiation at high temperatures. If the aim was to select these MAX phases to compose structural materials, an imminent challenge would be to produce them in a pure form. It is worth emphasizing that the MAX phases herein used for investigations were acquired from the US-based commercial company 3-ONE-2 LLC and the detailed characterization carried out using electron microscopy and XRD methods show that these materials are not single-phase, although the lamellae for the irradiation studies were lifted-out from the phase pure fields. Without the possibility to produce them in a pure form and in large scale to compose structural parts of nuclear reactors, at the present moment, it is impossible to judge whether the multiphase Ti-based MAX phases will be radiation tolerant or present suitable mechanical properties for such an application. Further studies are needed on this latter part.

Credit author statement

- Conceptualization and Visualization: MAT and PDE.
- Methodology, Investigation, Data Curation, Formal Analysis: MAT, SMD, JDAM, SPic, GG, LBC, JAV and PDE.
- Resources: GG, JAV, SPog, SF, SED, TAS and PDE.
- Supervision and Funding Acquisition: SF, OEA, SPog, SED, TAS and PDE.
- Writing Original Draft: MAT.
- Writing Review and Editing: All authors.
- Project administration: PDE.

Data availability

Data will be made available on request.

Declaration of competing interest

The authors declare that they have no known competing financial interests or personal relationships that could have appeared to influence the work reported in this paper.

Acknowledgments

MAT acknowledges research supported by the Laboratory Directed Research and Development (LDRD) program of the Los Alamos National Laboratory (LANL) under project number 20200689PRD2. Funding for this research was also provided through ASTRO, a United States Department of Energy workforce development program implemented at Oak Ridge National Laboratory through the Oak Ridge Institute for Science and Education under contract DE-AC05-06OR23100. PDE acknowledges funding from the U.S. Department of Energy, Fusion Energy Sciences. OEA acknowledges funding from his Early Career Program supported by LANL's LDRD under contract number 20210626ECR. The authors are grateful to the Engineering and Physical Sciences Research Council (EPRSC) for funding the MIAMI facilities under grants numbers EP/E017266/1 and EP/M028283/1 MAT and SPog would like to acknowledge the European Research Council (ERC) excellent science grant "TRANSDESIGN" funded via the Horizon 2020 program under contract 757961. With the warmest heart, MAT would like to dedicate this paper and the science herein to his daughter Sophie on the occasion of her birth in September 2022.

Appendix A. Supplementary data

Supplementary data to this article can be found online at https://doi.org/10.1016/j.mtener.2022.101186.

References

[1] W. Jeitschko, H. Nowotny, F. Benesovsky, Kohlenstoffhaltige ternäre verbindungen (h-phase), Monatsh. Chem. Verw. Teile. Anderer. Wiss. 94 (4) (1963) 672–676.
[2] W. Jeitschko, H. Nowotny, F. Benesovsky, Kohlenstoffhaltige ternäre Verbindungen (V-Ge-C, Nb-Ga-C, Ta-Ga-C, Ta-Ge-C, Cr-Ga-C und Cr-Ge-C), Monatsh. Chem. Verw. Teile. Anderer. Wiss. 94 (5) (1963) 844–850.
[3] W. Jeitschko, H. Nowotny, F. Benesovsky, Die H-Phasen: Ti2CdC, Ti2GaC, Ti2GaN, Ti2InN, Zr2InN und Nb2GaC, Monatsh. Chem. Verw. Teile. Anderer. Wiss. 95 (1) (1964) 178–179.
[4] W. Jeitschko, H. Nowotny, F. Benesovsky, Die H-Phasen Ti2TlC, Ti2PbC, Nb2InC, Nb2SnC und Ta2GaC, Monatsh. Chem. Verw. Teile. Anderer. Wiss. 95 (2) (1964) 431–435.
[5] W. Jeitschko, H. Nowotny, Die Kristallstruktur von Ti3SiC2 - ein neuer Komplexcarbid-Typ, Monatsh. Chem. Chem. Month. 98 (2) (1967) 329–337.
[6] M.W. Barsoum, T. El-Raghy, Synthesis and characterization of a remarkable ceramic: Ti3SiC2, J. Am. Ceram. Soc. 79 (7) (1996) 1953–1956.
[7] M. Barsoum, T. El-Raghy, Room-temperature ductile carbides, Metall. Mater. Trans. 30 (2) (1999) 363–369.
[8] M.W. Barsoum, T. El-Raghy, The MAX phases: unique new carbide and nitride materials: ternary ceramics turn out to be surprisingly soft and machinable, yet also heat-tolerant, strong and lightweight, Am. Sci. 89 (4) (2001) 334–343.
[9] M.W. Barsoum, MAX Phases: Properties of Machinable Ternary Carbides and Nitrides, John Wiley & Sons, 2013.
[10] M.W. Barsoum, M. Radovic, Elastic and mechanical properties of the max phases, Annu. Rev. Mater. Res. 41 (2011) 195–227.
[11] M.W. Barsoum, The mn+ 1axn phases: a new class of solids: thermodynamically stable nanolaminates, Prog. Solid State Chem. 28 (1–4) (2000) 201–281.
[12] Z. Sun, Progress in research and development on max phases: a family of layered ternary compounds, Int. Mater. Rev. 56 (3) (2011) 143–166.
[13] J. Gonzalez-Julian, Processing of MAX phases: from synthesis to applications, J. Am. Ceram. Soc. 104 (2) (2021) 659–690.
[14] M.A. Tunes, Transmission Electron Microscopy Study of Radiation Damage in Potential Nuclear Materials, Ph.D. thesis, University of Huddersfield, 2020.

[15] M.A. Tunes, V.M. Vishnyakov, O. Camara, G. Greaves, P.D. Edmondson, Y. Zhang, S.E. Donnelly, A candidate accident tolerant fuel system based on a highly concentrated alloy thin film, Mater. Today Energy 12 (2019) 356–362.
[16] O. El-Atwani, A. Alvarado, K. Unal, S. Fensin, J. Hinks, G. Greaves, J. Baldwin, S. Maloy, E. Martinez, Helium implantation damage resistance in nano-crystalline w-ta-v-cr high entropy alloys, Mater. Today Energy 19 (2021), 100599.
[17] S. Jin, H. Ma, E. Lu, L. Zhou, Q. Zhang, P. Fan, Q. Yan, D. Yuan, X. Cao, B. Wang, Depth distributions of cavities in advanced ferritic/martensitic and austenitic steels with high helium preimplantation and high damage level, Mater. Today Energy 20 (2021), 100687.
[18] D.J. Tallman, E.N. Hoffman, N.C. El'ad, B.L. Garcia-Diaz, G. Kohse, R.L. Sindelar, M.W. Barsoum, Effect of neutron irradiation on select MAX phases, Acta Mater. 85 (2015) 132–143.
[19] D.J. Tallman, L. He, B.L. Garcia-Diaz, E.N. Hoffman, G. Kohse, R.L. Sindelar, M.W. Barsoum, Effect of neutron irradiation on defect evolution in Ti3SiC2 and Ti2AlC, J. Nucl. Mater. 468 (2016) 194–206.
[20] D.J. Tallman, L. He, J. Gan, N.C. El'ad, E.N. Hoffman, M.W. Barsoum, Effects of neutron irradiation of Ti3SiC2 and Ti3AlC2 in the 121–1085C temperature range, J. Nucl. Mater. 484 (2017) 120–134.
[21] M.A. Tunes, R.W. Harrison, S.E. Donnelly, P.D. Edmondson, A transmission electron microscopy study of the neutron-irradiation response of Ti-based max phases at high temperatures, Acta Mater. 169 (2019) 237–247.
[22] K.R. Whittle, M.G. Blackford, R.D. Aughterson, S. Moricca, G.R. Lumpkin, D.P. Riley, N.J. Zaluzec, Radiation tolerance of Mn+1AXn phases, Ti3AlC2 and Ti3SiC2, Acta Mater. 58 (13) (2010) 4362–4368.
[23] X. Liu, M. Le Flem, J.-L. Béchade, F. Onimus, T. Cozzika, I. Monnet, XRD investigation of ion irradiated Ti3Si0.90Al0.10C2, Nucl. Instrum. Methods Phys. Res. Sect. B Beam Interact. Mater. Atoms 268 (5) (2010) 506–512.
[24] J. Nappé, I. Monnet, P. Grosseau, F. Audubert, B. Guilhot, M. Beauvy, M. Benabdesselam, L. Thomé, Structural changes induced by heavy ion irradiation in titanium silicon carbide, J. Nucl. Mater. 409 (1) (2011) 53–61.
[25] L. Zhang, Q. Qi, L. Shi, D. O'Connor, B. King, E. Kisi, D. Venkatachalam, Damage tolerance of Ti3SiC2 to high energy iodine irradiation, Appl. Surf. Sci. 258 (17) (2012) 6281–6287.
[26] S.C. Middleburgh, G.R. Lumpkin, D. Riley, Accommodation, accumulation, and migration of defects in Ti3SiC2 and Ti3AlC2 MAX phases, J. Am. Ceram. Soc. 96 (10) (2013) 3196–3201.
[27] L.F. Marion, I. Monnet, Saturation of irradiation damage in (Ti,Zr)3(Si,Al)C2 compounds, J. Nucl. Mater. 433 (1–3) (2013) 534–537.
[28] M. Imtyazuddin, A.H. Mir, M.A. Tunes, V.M. Vishnyakov, Radiation resistance and mechanical properties of magnetron-sputtered cr2alc thin films, J. Nucl. Mater. 526 (2019), 151742.
[29] H. Qarra, K. Knowles, M. Vickers, S. Akhmadaliev, K. Lambrinou, Heavy ion irradiation damage in zr2alc max phase, J. Nucl. Mater. 523 (2019) 1–9.
[30] D. Bowden, J. Ward, S. Middleburgh, S. de Moraes Shubeita, E. Zapata-Solvas, T. Lapauw, J. Vleugels, K. Lambrinou, W. Lee, M. Preuss, et al., The stability of irradiation-induced defects in Zr3AlC2, Nb4AlC3 and (Zr0.5,Ti0.5)3AlC2 MAX phase-based ceramics, Acta Mater. 183 (2020) 24–35.
[31] B. Tunca, G. Greaves, J.A. Hinks, P.Å. Persson, J. Vleugels, K. Lambrinou, In situ He+ irradiation of the double solid solution (Ti0.5,Zr0.5)2(Al0.5,Sn0.5)C MAX phase: defect evolution in the 350–800C temperature range, Acta Mater. 206 (2021), 116606.
[32] M.A. Tunes, M. Imtyazuddin, C. Kainz, S. Pogatscher, V.M. Vishnyakov, Deviating from the pure max phase concept: radiation-tolerant nanostructured dual-phase cr2alc, Sci. Adv. 7 (13) (2021), eabf6771.
[33] D. Clark, S.J. Zinkle, M.K. Patel, C.M. Parish, High temperature ion irradiation effects in max phase ceramics, Acta Mater. 105 (2016) 130–146.
[34] A. Chaklader, Reactive hot pressing, a new ceramic process, Nature 206 (4982) (1965) 392–393.
[35] M. Barsoum, T. El-Raghy, M. Ali, Processing and characterization of Ti2AlC, Ti2AlN, and Ti2AlC0.5N0.5, Metall. Mater. Trans. 31 (7) (2000) 1857–1865.
[36] Y. Zhou, F. Meng, J. Zhang, New MAX-phase compounds in the V–Cr–Al–C system, J. Am. Ceram. Soc. 91 (4) (2008) 1357–1360.
[37] W. Zhang, N. Travitzky, C. Hu, Y. Zhou, P. Greil, Reactive hot pressing and properties of Nb2AlC, J. Am. Ceram. Soc. 92 (10) (2009) 2396–2399.
[38] D.W. Clark, S.J. Zinkle, M.K. Patel, C.M. Parish, High temperature ion irradiation effects in MAX phase ceramics, Acta Mater. 105 (2016) 130–146.
[39] L. Giannuzzi, F. Stevie, A review of focused ion beam milling techniques for TEM specimen preparation, Micron 30 (3) (1999) 197–204.
[40] G. Greaves, A. Mir, R. Harrison, M. Tunes, S. Donnelly, J. Hinks, New microscope and ion accelerators for materials investigations (miami-2) system at the university of huddersfield, Nucl. Instrum. Methods Phys. Res. Sect. A Accel. Spectrom. Detect. Assoc. Equip. 931 (2019) 37–43.
[41] P.A. Burr, D. Horlait, W.E. Lee, Experimental and DFT investigation of (Cr,Ti) 3AlC2 MAX phases stability, Mater. Res. Lett. 5 (3) (2017) 144–157.
[42] J. Morgiel, J. Lis, R. Pampuch, Microstructure of Ti3SiC2-based ceramics, Mater. Lett. 27 (3) (1996) 85–89.
[43] D.A. Porter, K.E. Easterling, Phase Transformations in Metals and Alloys (Revised Reprint), CRC Press, 2009.
[44] D. Bandyopadhyay, R. Sharma, N. Chakraborti, The Ti-Al-C system (titanium-aluminum-carbon), J. Phase Equil. 21 (2) (2000) 195–198.
[45] S. Sambasivan, W. Petuskey, Phase relationships in the Ti–Si–C system at high pressures, J. Mater. Res. 7 (6) (1992) 1473–1479.
[46] W.E. Lee, E. Giorgi, R. Harrison, A. Maitre, O. Rapaud, Nuclear applications for ultra-high temperature ceramics and max phases, in: Ultra-High Temperature Ceramics: Materials for Extreme Environment Applications, 2014, pp. 391–415.
[47] S. Zinkle, G. Was, Materials challenges in nuclear energy, Acta Mater. 61 (3) (2013) 735–758.
[48] M.R. Gilbert, J.-C. Sublet, R.A. Forrest, Handbook of Activation, Transmutation, and Radiation Damage Properties of the Elements Simulated Using FISPACT-II and TENDL-2014; Magnetic Fusion Plants, CCFE-R(15)26, 2015, pp. 1–696.
[49] Y. Zhang, W.J. Weber, Ion irradiation and modification: the role of coupled electronic and nuclear energy dissipation and subsequent nonequilibrium processes in materials, Appl. Phys. Rev. 7 (4) (2020), 041307.
[50] Y. Zhang, H. Xue, E. Zarkadoula, R. Sachan, C. Ostrouchov, P. Liu, X.-l. Wang, S. Zhang, T.S. Wang, W.J. Weber, Coupled electronic and atomic effects on defect evolution in silicon carbide under ion irradiation, Curr. Opin. Solid State Mater. Sci. 21 (6) (2017) 285–298.
[51] J.A. Brinkman, On the nature of radiation damage in metals, J. Appl. Phys. 25 (8) (1954) 961–970.
[52] Y. Zhang, D.S. Aidhy, T. Varga, S. Moll, P.D. Edmondson, F. Namavar, K. Jin, C.N. Ostrouchov, W.J. Weber, The effect of electronic energy loss on irradiation-induced grain growth in nanocrystalline oxides, Phys. Chem. Chem. Phys. 16 (17) (2014) 8051–8059.
[53] S.H. Shah, P.D. Bristowe, Point defect formation in M2AlC MAX phases and their tendency to disorder and amorphize, Sci. Rep. 7 (2017) 1–8.
[54] S. Wooding, D. Bacon, W. Phythian, A computer simulation study of displacement cascades in alpha-titanium, Philosophical Magazine A 72 (1995) 1261–1279.
[55] R. Smallman, R. Bishop, Defects in solids, Mod. Phys. Metall. Mater. Eng. (1999) 84–124.
[56] C. Varvenne, F. Bruneval, M.C. Marinica, E. Clouet, Point defect modeling in materials: coupling ab initio and elasticity approaches, Phys. Rev. B Condens. Mater. Phys. 88 (2013), 134102.
[57] G. Verite, C. Domain, C.C. Fu, P. Gasca, A. Legris, F. Willaime, Self-interstitial defects in hexagonal close packed metals revisited: evidence for low-symmetry configurations in Ti, Zr, and Hf, Phys. Rev. B Condens. Mater. Phys. 87 (2013), 134108.
[58] R. Qiu, H. Lu, B. Ao, L. Huang, T. Tang, P. Chen, Energetics of point defects in aluminum via orbital-free density functional theory, Phil. Mag. 97 (2016) 2164–2181.
[59] P.-W. Ma, S. Dudarev, Nonuniversal structure of point defects in face-centered cubic metals, Phys. Rev. Mater. 5 (1) (2021), 013601.
[60] G. Odette, T. Yamamoto, D. Klingensmith, On the effect of dose rate on irradiation hardening of RPV steels, Phil. Mag. 85 (2005) 779–797.
[61] M. Hernandez-Mayoral, C. Heintze, E. Onorbe, Transmission electron microscopy investigation of the microstructure of Fe-Cr alloys induced by neutron and ion irradiation at 300C, J. Nucl. Mater. 474 (2016) 88–98.
[62] H. Ke, P. Wells, P.D. Edmondson, N. Almirall, L. Barnard, G.R. Odette, D. Morgan, Thermodynamic and kinetic modeling of Mn-Ni-Si precipitates in low-Cu reactor pressure vessel steels, Acta Mater. 138 (2017) 10–26.
[63] E.R. Reese, N. Almirall, T. Yamamoto, S. Tumey, G.R. Odette, E.A. Marquis, Dose rate dependence of Cr precipitation in an ion-irradiated Fe-18Cr alloy, Scripta Mater. 146 (2018) 213–217.
[64] S. Shu, N. Almirall, P.B. Wells, T. Yamamoto, G.R. Odette, D.D. Morgan, Precipitation in Fe-Cu and Fe-Cu-Mn model alloys under irradiation: dose rate effects, Acta Mater. 157 (2018) 72–82.

Dr. Matheus A. Tunes is currently Director's Fellow of the Materials Science and Technology Division at the Los Alamos National Laboratory, United States. He is an experimental physicist graduated from the Institute of Physics at the University of São Paulo, Brazil. In 2020, he received his PhD in Atomic Collision in Solids from the MIAMI Facilities at the University of Huddersfield, United Kingdom. His research is on fundamental material's thermodynamics, and it is currently focused in to understand, characterize and optimize the response of materials subjected to extreme environments: high-temperature, corrosion, and irradiation.

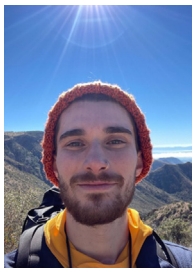

Sean Drewry is currently a PhD student at the University of Tennessee Knoxville in the Materials Science and Engineering department. He received a BSc in Nuclear Engineering from Missouri University of Science and Technology. His PhD research focuses on synthesis and characterization of ceramics for nuclear applications. This has included areas of research into complex mineral phases and different uranium-based nuclear fuel forms.

Professor Stefan Pogatscher is currently Head of the Department of Metallurgy at the Montanuniversität Leoben, Austria. He received his PhD from the same university in 2012 and was a post-doc at ETH Zurich, Switzerland, from 2012 to 2015. Since 2015, Pogatscher has been back at Montanuniversität Leoben, initially as an assistant and associate professor, and from 2020 as a full professor. His research focuses on the metallurgy of sustainable light metals and high-resolution material characterization.

Dr. Tarik A Saleh is the deputy group leader of the Materials Science in Radiation and Dynamic Extremes group at Los Alamos National Laboratory, a group consisting of 90 materials scientists, post-docs, students, and support staff. Over his 19 years at Los Alamos, he has worked on thermophysical and thermomechanical properties of fuels, actinides, and irradiated cladding materials. He specializes in acoustic and other novel characterization of advanced materials. He received his PhD in materials science from the University of Tennessee, Knoxville in 2006, along with an MEng from UC Berkeley in 2000 and a BS from MIT in 1995.

Professor Philip Edmondson currently holds the UKAEA Chair in Tritium Science & Technology within the Department of Materials at the University of Manchester, UK. Prior to this, he was a Senior Staff Scientist and Group Leader at Oak Ridge National Laboratory, United States. His research is centered around the behavior of hydrogen isotopes within materials and the tritium fuel cycle for nuclear fusion applications; and the interactions of charged particles with matter, specifically the defect/damage formation and recovery in materials in support of nuclear energy issues.